Thermal Science and Applications
https://www.sciltp.com/journals/tsa

Article

Study on the Triple Integration of Solar Chimney, Solar Still, and CSP System to Promote Sustainable Power and Desalinated Water Production

Mohammad Sajjadi [1,*], Mohammad Reza Yousefi [2], Mansour Shirvani [3] and Yasaman Bozorgzad [4]

[1] Faculty of Engineering and Applied Science, University of Regina, 3737 Wascana Parkway, Regina, SK S4S 0A2, Canada
[2] School of Chemical Engineering, University of Zanjan, University Blvd., Zanjan 45371-38791, Iran
[3] School of Chemical Engineering, Iran University of Science & Technology, Narmak, Tehran 16846-13114, Iran
[4] School of Sustainable Energy Engineering, Simon Fraser University, 10285 University Drive Surrey, Surrey, BC V3T 0N1, Canada
* Correspondence: mohammad.sajjadi@uregina.ca

How To Cite: Sajjadi, M.; Yousefi, M.R.; Shirvani, M.; et al. Study on the Triple Integration of Solar Chimney, Solar Still, and CSP System to Promote Sustainable Power and Desalinated Water Production. *Thermal Science and Applications* **2026**, *1*(2), 200–214. https://doi.org/10.53941/tsa.2026.100013

Received: 26 February 2026
Revised: 11 June 2026
Accepted: 12 June 2026
Published: 23 June 2026

Abstract: Mitigating the consequences of global warming on the shortage of water and sustainable energy requires clean technologies, such as solar energy systems. In this regard, integrating multiple clean technologies can provide an effective solution for simultaneous sustainable energy and freshwater production. In this study, a novel hybrid system integrating a Solar Chimney Power Plant (SCPP), solar still, and Concentrated Solar Power (CSP) system are proposed and numerically investigated. The proposed design lies in utilizing the CSP system as an auxiliary thermal energy source to enhance both airflow inside the chimney and evaporation inside the solar still simultaneously. Conducted computational Fluid Dynamics Analysis (CFD) for a system comprised of a 12 m height chimney and 3.4 m solar collector, accompanied by solar still basins located under the transparent collector, and the added CSP system showed that the basin temperature reached approximately 72 °C, and the water temperature in the collector outlet increased to about 62 °C in the triple system. Also, the chimney inlet velocity reached 2.2 m/s. The power generated in the new design showed a 68.2% increase via producing 0.64 W compared to the base case; meanwhile, the water production was 7554 g, indicating 18% rise in desalination capability. The observed results highlighted the substantial impact of additional thermal energy on system performance obtained from the CSP system compared to conventional hybrid systems.

Keywords: solar chimney; solar still; CSP system; sustainable electricity and water

1. Introduction

Over the past few decades, there has been a significant growth in the need for energy, which has presented human civilizations with many issues, including global warming [1]. The rise in energy demand has diverse factors, from population growth and industrial development to modern lifestyle, which, as a ripple effect, led to a noticeable increase in water consumption as well [2]. Moreover, climate change poses significant challenges for water security, especially for regions suffering severe drought in recent years [3]. In this regard, human society is at a turning point in the energy and water provision in this century. Accordingly, the rising worldwide energy and clean water consumption have signified the important role of clean energy sources like solar energy systems as one of the main promising solutions for tackling global warming repercussions in terms of water and electricity shortage.

It is evident that because of the innately pure and long-lasting superior qualities of clean energies, they are not only readily available substitutes for fossil fuels but also greatly safeguard the environment. This idea has clearly inspired a lot of scholars to advance technology and implement useful measures in this field [4]. Meanwhile, the most recent thermometry research conducted in 2024 revealed that global warming has surpassed the 1.5 °C threshold that defines the climate targets outlined in the Paris Agreement, far sooner than anticipated [5]. Therefore, for achieving sustainable energy production and proper access to water sources, research activities for finding appropriate solutions, including optimization of current technologies and developing hybrid systems, should be promoted.

In this regard, the Solar Chimney Power Plant (SCPP), initially suggested by Cabanyes, is one of the underdeveloped methods to accomplish electricity generation from renewable energy [6]. SCPP includes a chimney, a collector with a clear roof, and a power-generating device at the base of the chimney, as can be observed in Figure 1. Solar radiation warms the airflow beneath the glass collector [7]. Consequently, the rising air flow toward the chimney is produced by the buoyancy effect between heated air streams and the surrounding air due to the density difference [8]. This phenomenon is accelerated by the tower's strong updraft conditions, which speed up air movement. The turbine next to the chimney transforms the kinetic energy of the airflow into mechanical energy as it moves through the system.

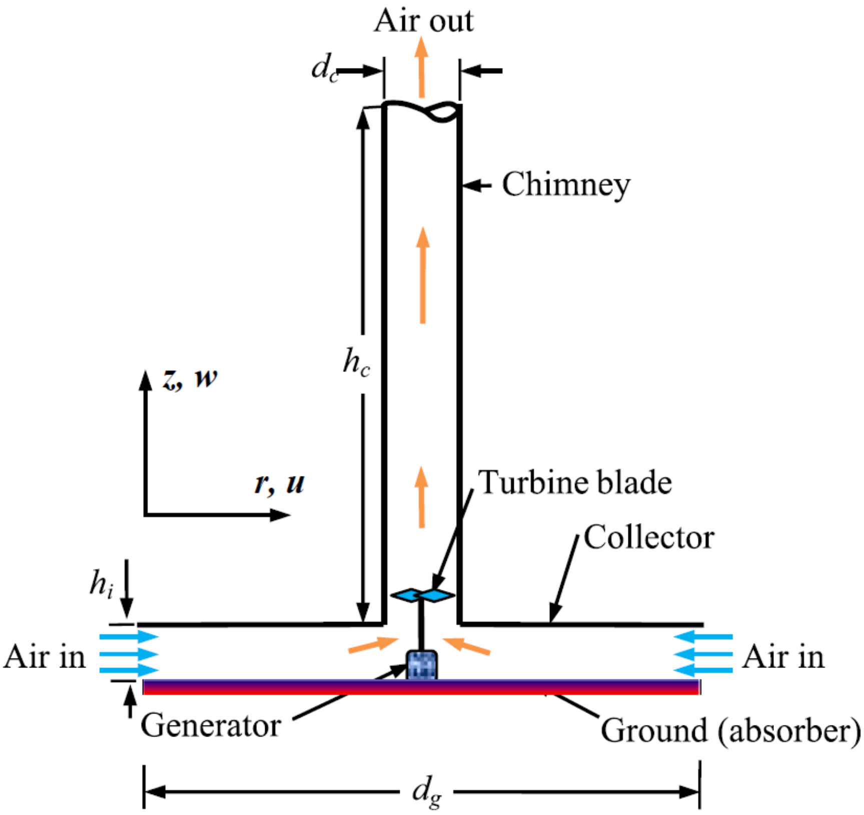

Figure 1. Schematic for solar chimney power plant. Reprinted with permission from Ref. [7].

In 1981, Schlaich investigated the operation of the first Solar Chimney Power Plant (SCPP) [9]. Afterwards, a prototype plant with a 244 m collector diameter and a 194 m chimney height was constructed to produce 50 KW of electricity. It is noteworthy that numerous analytical and experimental studies have been conducted in recent years to evaluate the efficacy of solar chimney systems, where the performance can be impacted by material and thermal storage, system design arrangement, integration with other clean technologies, and climate conditions [10]. Ghalamchi et al. compared five different theoretical models regarding the effects of collector radius and its inlet height, chimney height, and solar radiation on the performance of solar chimney systems. The results demonstrated that larger canopy diameter and column height led to a notable increase in the intended system's energy production [11]. The results demonstrated that larger canopy diameter and column height led to a notable increase in the intended system's energy production. In 2016, a numerical study was conducted for the analysis of a solar chimney with an inclined collector roof [12]. The results showed that changes in the collector-roof inclination increase the mass flow rate of the system. Raising the outlet collector height while maintaining the intake collector height results in a higher power output in SCPP. The impacts of the double roof collector with the co-current and counter-current flow arrangement on the system's overall performance were assessed in 2020 by Nasraoui et al. [13]. They demonstrated that a dual roof collector with a counter-flow configuration may increase the solar chimney power plant's overall efficiency. In another study, a theoretical model was created by Al-Abadi et al. [14] to determine how well a SCPP with a black concrete base would absorb and retain more heat at night. According to the findings, black concrete improved heat storage at night, which enhanced energy production. Afsari et al. [15] examined the impacts of increasing air volume and soil layer in 2024 for a built pilot setup of SCPP with a 12 m chimney height under five distinct scenarios. The inclusion of a soil layer enabled the system to have thermal storage, which produced an airflow velocity of 0.2 m/s at the beginning of the night, according to the findings of the experiments and simulations. While more air height inside the collector might result in a fall in flow velocity, the soil layer saw a slight decrease in airflow velocity over the day. Additionally, Li et al. looked into the impacts of using Phase Change Materials (PCM) as a thermal storage section for the solar chimney plant collector [16]. The improved airflow rate and temperature difference were observed from their study.

In addition, it is said that because of the low productivity and the substantial amount of space needed for construction, combining solar chimney and other technologies may be beneficial, although few experimental studies have been conducted for combined systems [17]. In this regard, Mokrani and his colleagues carried out experimental studies on hybrid power plants that included geothermal water and solar chimney electricity. Their findings indicated an improvement in the system's overall performance by means of intended integration with geothermal energy [18]. Similarly, Sing et al. assessed the combination of photovoltaic systems (PV) with solar chimney power plants to improve ultimate power generation. [19]. Additionally, another research by Abdelsalam et al. suggested combining a solar chimney power plant with an electrolysis station to produce green hydrogen [20]. The findings showed that the SCPP is now competitive with other energy production facilities since its Levelized Cost of Energy (LCOE) has improved to 0.51 $/kWh as a consequence of the income generated from the production of H_2 and O_2. In a different study, Sajjadi et al. suggested integrating a solar chimney with a CSP system to supply an extra heat source as a supplementary driving force in SCPP, increasing airflow velocity [21]. The study's findings indicated that the secondary heat source improved overall performance and, in comparison to conventional designs, this innovation increased the possibility of producing power at night significantly. This was because the collector canopy's temperature difference from the surrounding air was higher.

On the other hand, it is suggested that merging solar chimney and solar still systems might be beneficial due to poor productivity and the huge building space required for both. However, few experimental studies have examined the proposed hybrid design [22]. The solar still consists of three primary components: the raw water basin, the glass roof, and the collecting channel, which are shown in Figure 2 By capturing evaporating droplets and condensing them into its distillation channel, sun radiation is used to directly distill saline or brackish water [23]. In order to produce clean water and power at the same time, Zue et al. experimentally evaluated a combined solar chimney and desalination system in 2012 [24]. It was discovered that the primary time to produce distilled water occurs when there is no sunlight. In the meantime, the first third of the heat collector experiences the greatest temperature rise. Mostafa et al. [25] conducted experimental studies for this hybrid system, demonstrating that increased salt content inside the systems had a detrimental influence on the system's overall productivity. Meanwhile, increasing salt concentrations lead to greater thermal energy storage during sunny hours. Long et al. published research on the efficacy of liquid desiccant regeneration in solar stills and natural convective regenerators, with and without the mixed convection effect created by solar chimneys [26]. Its findings revealed that the improved mass transfer efficiency caused by mixed convection created by the solar chimney is obvious. Kabeel et al. [27]. concentrated their study on boosting the temperature of the water while simultaneously reducing the temperature of the glass cover, which had a substantial influence on the overall performance of the production process. In recent studies, other aspects of solar desalination have been reviewed as well. Huang et al. [28] studied a multifunctional photothermal evaporator based on a black g-C_3N_4 hydrogel. Their research showed how photothermal materials can boost sun absorption and interfacial evaporation processes, which improves desalination and water purification efficiency. These advancements highlight the significance of effective solar-to-thermal energy conversion, which can be used in solar still systems to improve desalination efficiency and freshwater yield.

Afsari and his colleagues presented a detailed experimental investigation on a hybrid solar chimney system and solar still in 2023, demonstrating the potential for producing power and water at the same time [29]. Their findings revealed through experimentation that the intended combination with a water desalination system caused the peak times for temperature and velocity profiles among collectors to diverge from those of the typical solar chimney design.

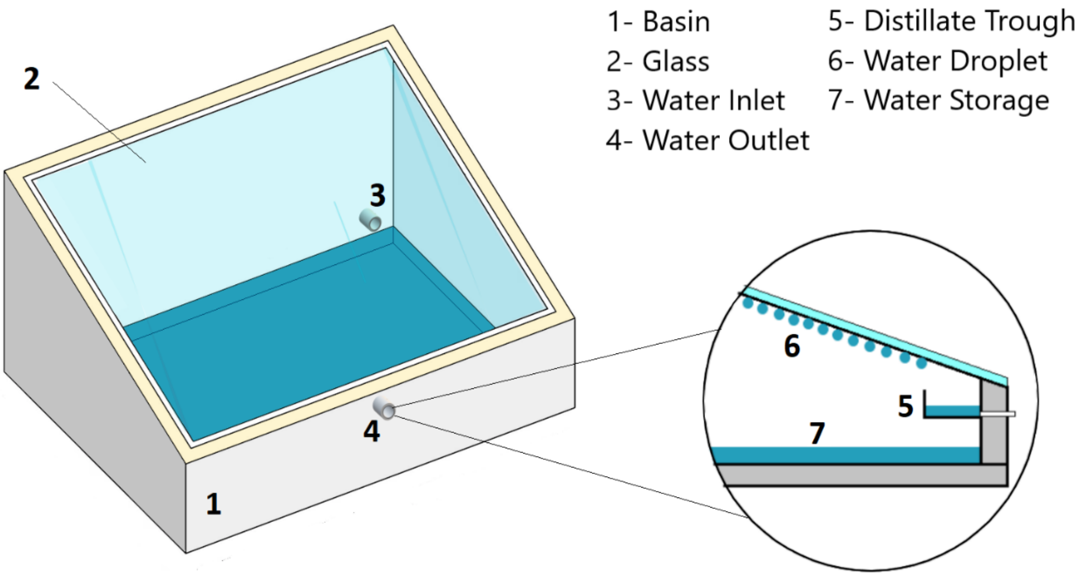

Figure 2. Solar still water desalination system [29].

Therefore, it is clarified in previous studies that hybrid solar chimney and solar still can produce simultaneous water and electricity, which would be considered as a promising solution to achieve sustainability in remote areas, although this hybrid system needs improvement in various aspects, and thermal performance is one of the main topics.

Accordingly, in this study, the authors tried to introduce the possibility of overall performance improvement by a novel triple integration of solar chimney, solar still, and CSP system. The novelty of the proposed arrangement illustrated that the capability of the CSP system can promote heat distribution among system. Not only did it provide more desalinated water, but it also generated far more kinetic energy compared to previous combinations or conventional designs. Accordingly, to further understand the impact of the intended secondary heat source on the production of electricity and desalinated water, a Computational Fluid Dynamics study (CFD) was carried out.

2. Methodology and Design Development

2.1. Hybrid System Description

The proposed triple hybrid design is indicated in Figure 3, comprising a solar chimney, a solar still, and Solar Concentrated Power System (CSP). This hybrid design arrangement presents a novel approach to enhancing sustainable energy generation and desalinated water production. This triple-integration strategy leverages the strengths of each component to maximize efficiency and resource utilization. The solar concentrator system warms a heat-transferring fluid medium, as seen in Figure 3. A thermal storage tank can be used to store it if needed. TES is made to concurrently control the heat-transferring fluid's flow rate and save energy. The circulation of the heat-transfer fluid requires pumping systems whose operational efficiency can significantly influence the overall performance of thermal-fluid systems. Previous studies have investigated the efficiency characteristics of pumping systems operating with different motor technologies under thermal-fluid applications [30]. Heat is transferred to the air under the canopy and to the wall of the basin by the hot fluid that is injected into the center of the collector and circulates helically inside the circular coils. The coils are embedded within the sand layer; therefore, heat is transferred indirectly to the basin water through conduction across the basin bottom wall and the surrounding sand medium. Simultaneously, part of the transferred thermal energy increases the air temperature beneath the collector canopy. Although the sand layer introduces additional thermal resistance, it improves thermal storage capability and promotes more uniform temperature distribution within the system. After leaving the collector's edge, it is recycled back into the CSP system. Additionally, a layer of insulation beneath the tubes can stop excessive heat loss to the earth.

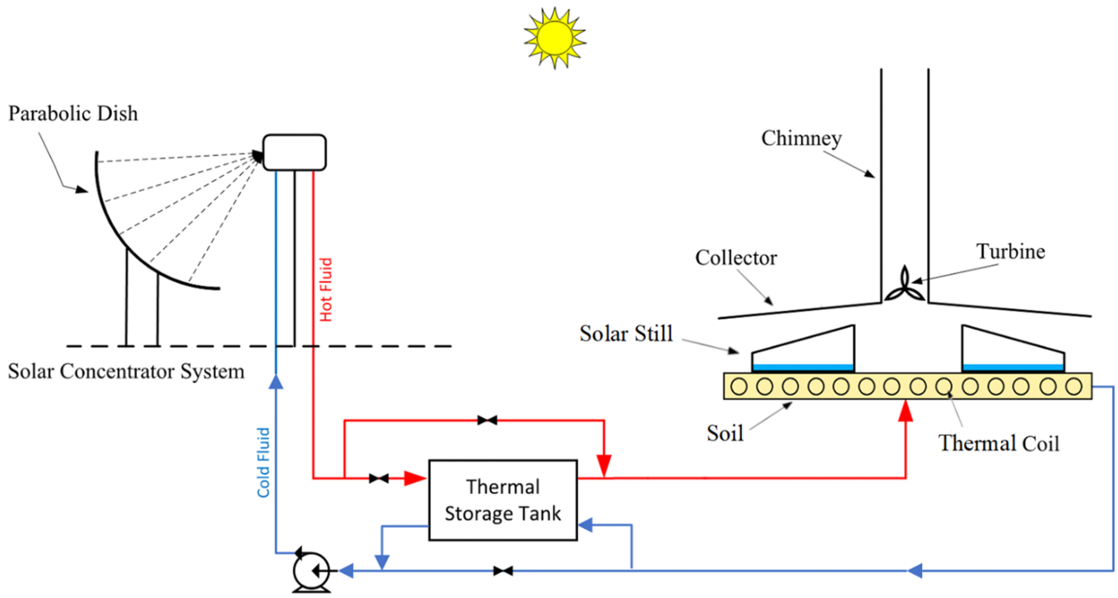

Figure 3. Proposed design for triple integration of solar chimney, solar still, and CSP system.

Additionally, sand is placed in the area between the heat transmission pipes to improve thermal storage and temperature dispersion. As a result, the new proposed design raises the temperature and velocity of the air inside the collector to produce more power, which is accompanied by a faster rate of water production. Additionally, it ensures improved performance while the system is operating at night. In other words, enhancing the collector's thermal performance via the suggested innovation results in achieving the same power output with a smaller plant scale compared to traditional design, which also represents an economic achievement for lowering the costs. Moreover, considering the thermal potential of the heat-transfer fluid in the CSP system, several opportunities exist to further enhance the performance of the solar chimney. For example, a practical application of the proposed design is the use of return heat-transfer fluid, such as steam condensate, from an existing CSP plant, which can provide additional power generation for the SCPP.

2.2. Base Case Experimental Setup for Validation

In this regard, the simulation has been done to analyze the notion of triple integration, and it is validated based on the authors' previous experimental research, which provides a combination of solar still and solar chimney. In order to assess the efficacy of the combined system in the current study, a pilot-scale solar chimney of 12 m in height and 3.4 m in collector diameter was built in Tehran, as seen in Figure 4. It was integrated with eight solar water basins. Table 1 provides a summary of the system geometry.

Table 1. Geometric parameters of constructed solar chimney [29].

Geometric Parameter	Dimensions
Diameter of the chimney	25 cm
Height of chimney	12 m
Diameter of collector	3.4 m
Air entrance gap at collector	6 cm
Collector sidewall height	60 cm
Rear wall height of the basin	30 cm
Front wall height of the basin	10 cm

To prevent heat loss, a 3 cm layer of glass-wool insulation was placed on the ground under the canopy, and the chimney was insulated with 2 cm of mineral fiber. Furthermore, the collector's canopy's transparent plastic material offered roughly 70% transparency. In order to reduce the impact of wind on the measured data, a protective plastic coating was also placed around the collector's entrance. At the setup location (Lat/Lon: 35.741, 51.511), the global radiation was recorded close to 900 W/m^2, which was valid when compared to the pertinent databases. The collector's initial midsection was where the stills were placed. Originally, the basin's roof was made of glass and sloped 15 degrees to allow for adequate drainage as condensed droplets flowed into the distillate collection. To make an appropriate environment in the water basin for better evaporation of water, the walls of the still were insulated. Under the measured peak solar radiation conditions of approximately 900 W/m^2, the experimental base case produced an airflow velocity of about 2 m/s at the chimney inlet, while the collector outlet temperature and basin water temperature reached approximately 59.2 °C and 73 °C, respectively. These measured values were later used for validation of the numerical CFD model.

Figure 4. Solar Chimney setup in Iran University of Science & Technology, Tehran [29].

2.3. Numerical Model Description

The hybrid solar chimney and solar desalination system's governing equations, which include the continuity, momentum, and energy equations, are generally as follows [31]:

Mass conservation:

$$\frac{1}{r}\frac{\partial(rpu)}{\partial r}+\frac{\partial(pv)}{\partial z}=0 \tag{1}$$

Momentum conservation

$$\rho\left(\frac{\partial u}{\partial t}+u\frac{\partial u}{\partial r}+v\frac{\partial u}{\partial z}\right)=-\frac{\partial p}{\partial r}+\mu\left[-\frac{u}{r^2}+\frac{1}{r}\frac{\partial}{\partial r}\left(r\frac{\partial u}{\partial r}\right)+\frac{\partial^2 u}{\partial z^2}\right] \tag{2}$$

$$\rho\left(\frac{\partial v}{\partial t}+u\frac{\partial v}{\partial r}+v\frac{\partial v}{\partial z}\right)=\frac{\partial p}{\partial z}+\mu\left[\frac{1}{r}\frac{\partial}{\partial r}\left(r\frac{\partial v}{\partial r}\right)+\frac{\partial^2 v}{\partial z^2}\right]+\rho g_z \tag{3}$$

Energy conservation:

$$\rho c_P\left[\frac{\partial T}{\partial t}+\frac{1}{r}\frac{\partial}{\partial r}(rTu)+\frac{\partial}{\partial z}(Tv)\right]=\frac{1}{r}\frac{\partial}{\partial r}\left(rk\frac{\partial T}{\partial r}\right)+\frac{\partial}{\partial z}\left(wk\frac{\partial T}{\partial z}\right)+\frac{\partial p}{\partial t}+\frac{1}{r}\frac{\partial}{\partial r}(rPu)+\frac{\partial}{\partial z}(Pv)+\Phi \tag{4}$$

The Rayleigh Number (*Ra*) is applicable to use for assessing the system's turbulence level because the solar chimney system relies on buoyancy-driven flow [32].

$$Ra=\frac{g\beta\Delta T L^3\rho}{\mu a} \tag{5}$$

According to earlier research, the *Ra* indicates the air stream turbulence for the solar chimney, and when it is larger than 10^{10}, it indicates that the natural convection flow has transformed into a turbulent one.

Additionally, the desalination part of the hybrid system is regarded as a traditional solar still in earlier numerical calculations, except for its roof, which is in contact with airflow amid the collection canopy. There is consensus among previous studies to use Dunkel's heat and mass transfer laws for solar stills because there isn't a precise numerical model created for the planned hybrid system. However, it should be acknowledged that applying this model to a coupled hybrid system involving CSP-assisted heating and enhanced airflow may introduce additional uncertainties [33,34].

Based on the Dunkel mathematical model, the heat transfer from the water surface to the overlying glass cover can be determined using Equation (6).

$$q_{e.w}=h_{ev.w.w-g}\left(T_w-T_g\right) \tag{6}$$

where T_w and T_g are the temperatures of the water and the glass roof, respectively.

Equation (7) is used to calculate the total evaporative heat transfer coefficient between the saline water and the still roof, with P_w and P_g denoting the water vapor partial pressures at the basin temperature and the glass temperature, respectively.

$$h_{ev.w-g} = 0.016273 \times h_{c.w-g} \frac{(P_w - P_g)}{(T_w - T_g)} \tag{7}$$

$$P_w = exp\left(25.317 - \frac{5144}{T_w + 273}\right) \tag{8}$$

$$P_g = exp\left(25.317 - \frac{5144}{T_g + 273}\right) \tag{9}$$

$h_{c,w\text{-}g}$ is the convective heat transfer coefficient between the desalination roof and, which is determined via Equation (10)

$$h_{c.w-g} = \frac{Nu.k_{air}}{d} = C(GrPr)^n \tag{10}$$

where working conditions and plant dimensions are needed to obtain C and n values and dimensions of the desalination plant. According to the Dunkel model, C = 0.075 and n = 1/3 were proposed. Accordingly, the following relation was obtained from Equation (6):

$$h_{ev.w-g} = 0.884 \times \left[(T_w - T_g) + \frac{(P_w - P_g)(T_w + 273)}{268.9 \times 10^3 - P_w}\right]^{1/3} \tag{11}$$

Therefore, Equation (12) provides the amount of freshwater production, where h_{fg} is the latent heat of vaporization, and A_w is the water surface area:

$$\dot{m}_{hourly}\left(\frac{kg}{h}\right) = \frac{q_{e.w}}{h_{fg}} \times 3600 \times A_w \tag{12}$$

2.3. Numerical and CFD Simulation

The performance of the hybrid system has been simulated in the current study using a 2D numerical model created in ANSYS-Fluent Version 2021. A complex thermodynamic and fluid dynamic mathematical model, made feasible by Computational Fluid Dynamics (CFD), a tried-and-true method for simulating fluid behavior in a variety of systems, including SCPP and hybrid systems, may provide extensive analysis.

The Boussinesq hypothesis for density was considered to be true for the solar chimney system, as verified in previous publications [35]. Additionally, the discrete ordinates model (DOM) was chosen for the radiation phenomena present in the system chimney, water, and collector sections. The Quad/Tri meshing approach was used to discretize each. Additionally, an independent study on meshing has been carried out to help authors choose models with the fewest possible numerical errors. In simulation calculations, the chimney, the ground area, and the basin side walls are considered as adiabatic bounds since they are insulated by glass wool. Additionally, calculations for the collector's surrounding walls and the transparent canopy's outside surface assume a constant temperature of 317 °K with h = 8 W/m^2. Additionally, 800 W/m^2 is the global solar radiation utilized in computations. Since it was close to the highest radiation recorded at the setup position (Lat/Lon: 35.741, 51.511) in Tehran city, it was chosen as a typical value based on the experiment's obtained data. Both the collector input flow and the chimney output flow models employ the atmospheric value assumption for the static pressure. Table 2 provides a summary of the desired simulation's boundary conditions.

Table 2. Boundary conditions for CFD simulation.

Description	Type	Surface Condition
Ground	Wall	Adiabatic
Basin Body	Wall	Adiabatic
Collector roof	Wall	900 (W/m^2)
Chimney	Wall	Adiabatic
Side Wall	Wall	T = 317 °K, h = 8 (W/m^2·K)
Inlet	Pressure-inlet	P (atm)
Outlet	Pressure-outlet	P (atm)

In the current work, the simulation model has been generated and validated by the outcomes of the intended experimental result, which is called in this paper the base case. The performance of a solar chimney with a supplementary heat source, such as a CSP system, was then assessed for the same ambient conditions. In this regard, it is assumed that the provided power input delivered by the CSP system is equivalent to 30 kg/h and 60 kg/h of water stream with 20 °C increased temperature, which will be called design case 1 and design case 2, respectively.

2.4. Simulation Validation

The simulation results for various operational parameters, such as collector outlet temperature, water temperature in basins, and air velocity at the chimney's entrance, have been validated via comparison with obtained experimental information, in which proper trends were achieved. The results of this comparison are highlighted in Table 3.

Table 3. Simulation validation.

Description	Collector's Outlet Temperature	Water Temperature in the Basin	Chimney Entrance Airflow Velocity	Water Production in the Basin
Experimental Data	59.2 °C	73 °C	2 m/s	110 g
Simulation Results	59 °C	72 °C	1.9 m/s	121 g

Additionally, a mesh independent study was carried out to find the minimum error in model convergence. It was obvious that rising the mesh number can lead to an increase in the computation time and related expenses. In the meantime, Figure 5 shows the minimal error point, which is the ideal one to employ in further computations. Consequently, a grid of 291,600 cells overall produced the least amount of simulation error.

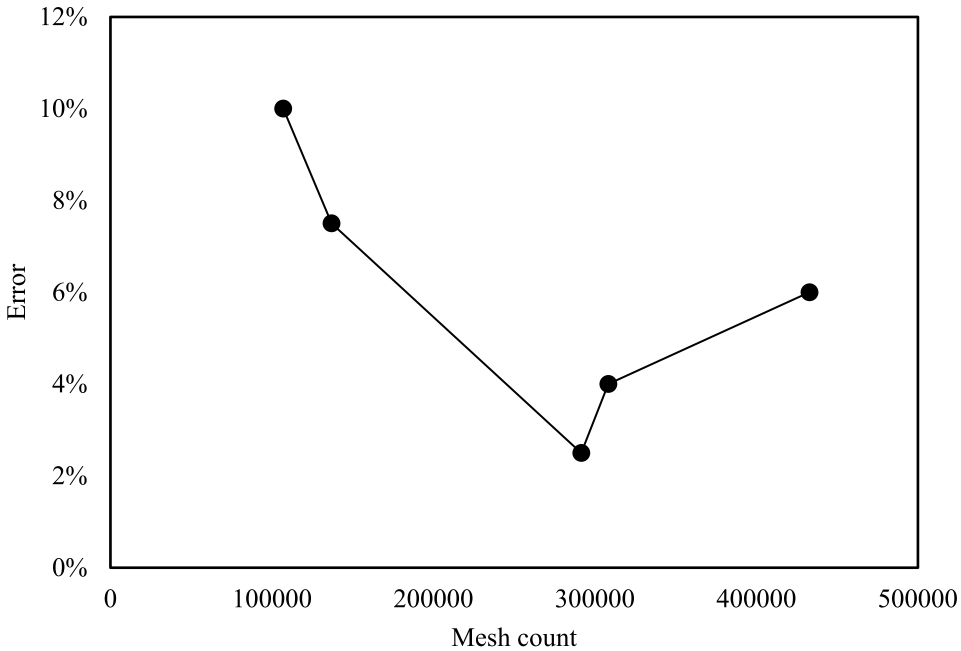

Figure 5. Grid sensitivity results.

3. Results and Discussion

In order to conduct numerical CFD simulations, a 2D axisymmetric model of SCPP has been defined in Fluent. The Quad/tri meshing method was used to mesh the geometry. Figures 6 and 7 displayed the contour plots for temperature and velocity within the system, respectively.

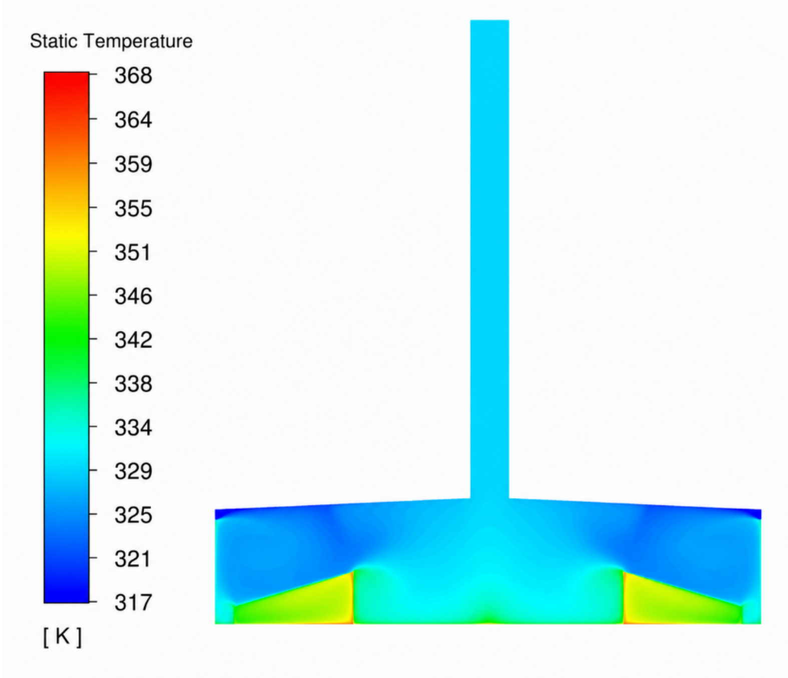

Figure 6. Contour plot for temperature profile in the system.

The air temperature rose throughout the collection, as shown in Figure 6, and eventually reached its maximum of 59 °C at the interface between the chimney inlet and the collector's output zone. Additionally, it was noted that the air velocity reached 2 m/s, as seen in Figure 7. It should be noted that these conclusions are consistent with the experimental data from the authors' earlier study shows that the numerical work was validated.

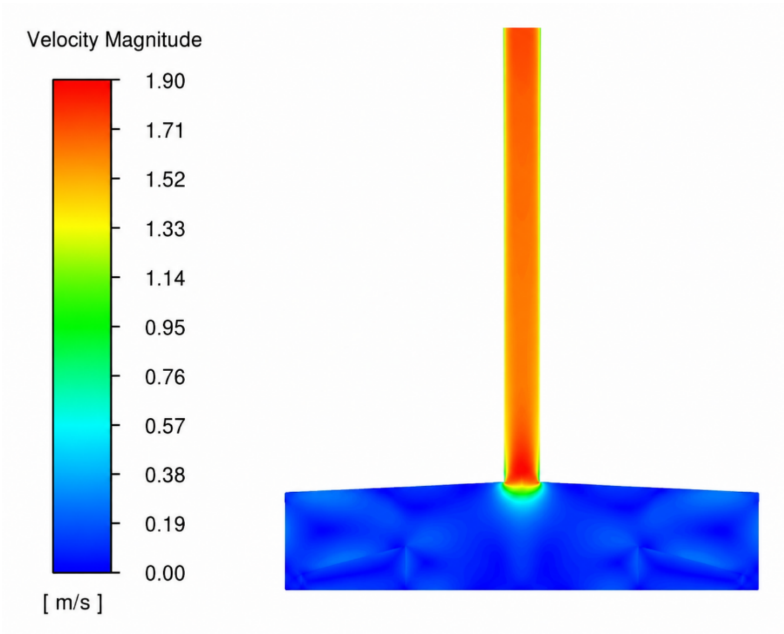

Figure 7. Contour plot for velocity profile in the system.

The provided comparative data in Figure 8 illustrate the temperature profiles of a hybrid solar chimney power plant (SCPP) and solar still system under three different scenarios: the base case, new design 1, and new design 2. This study examined the impact of integrating a Concentrated Solar Power (CSP) system as a secondary heat source to enhance the overall performance of the hybrid system, focusing on the simultaneous production of electricity and desalinated water. The base case represents the initial setup, validated by experimental results, while the new designs involve additional thermal energy inputs from the CSP system. Specifically, new design 1 and new design 2 simulate the effects of introducing a water stream heated by 20 °C at flow rates of 30 kg/h and 60 kg/h, respectively. As illustrated in Figure 8, the basin water temperature is approximately 72 °C, and the water temperature in the collector outlet is around 58 °C. When the CSP system is introduced in new design 1, the collector outlet temperature remains relatively stable at around 72 °C, but the water temperature in the basin increases to approximately 59 °C. This indicates that the additional thermal energy from the CSP system raises the basin water temperature, enhancing the evaporation rate and, consequently, the desalination process. In new design 2, with a higher water flow rate of 60 kg/h, the water temperature hovers around 78 °C, but the water temperature in the collector increases to approximately 61 °C, suggesting an even more significant boost in desalination efficiency.

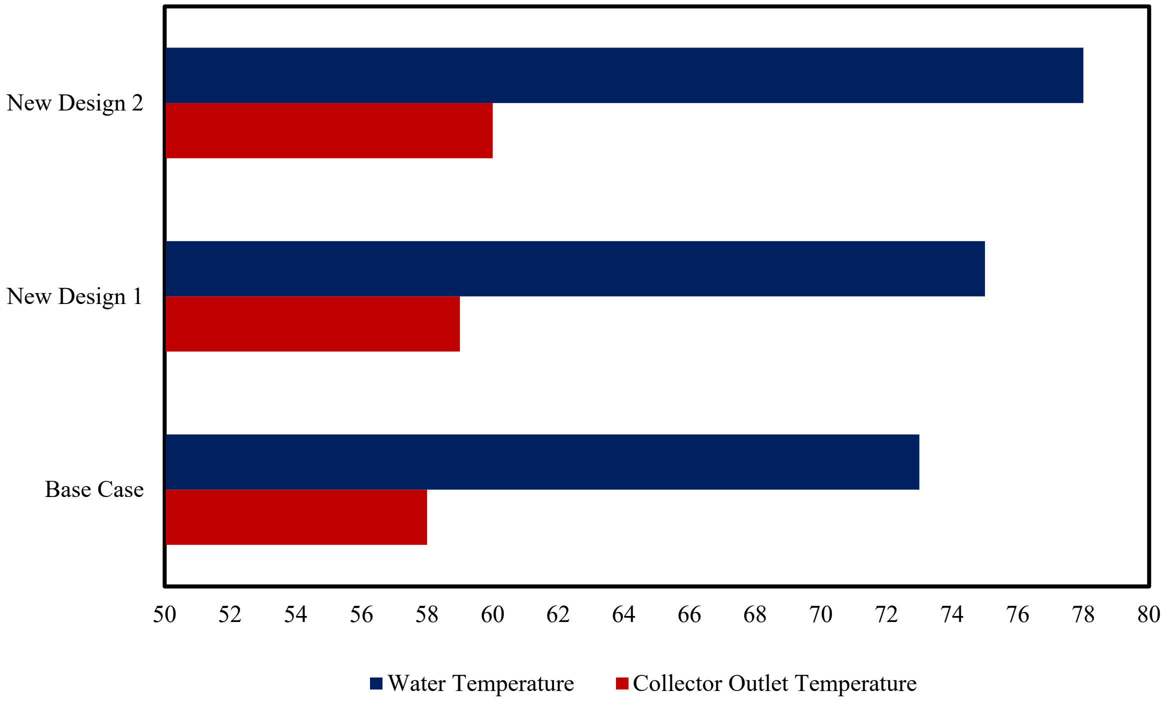

Figure 8. Collector outlet temperature in different cases.

The observed increase in water and electricity production in the new designs can be attributed to the enhanced thermal energy input from the CSP system. By preheating the water stream before it enters the solar chimney system, the overall thermal efficiency is improved, leading to higher temperatures in the basin. This temperature rise accelerates the evaporation process, resulting in increased freshwater production. Simultaneously, the higher temperatures at the collector outlet enhance the thermal updraft within the solar chimney, driving the turbine more effectively and generating more electricity. The combination of these factors demonstrates the synergistic effect of integrating a CSP system with a hybrid SCPP and solar still, providing a practical solution for improving the performance and output of renewable energy and desalination systems.

Figure 9 presents the water production performance of the hybrid solar chimney power plant (SCPP) and solar still system under three scenarios: the base case, new design 1, and new design 2. This chart complements the previous temperature profile analysis by quantifying the amount of desalinated water produced in each case. The base case yields a water production of 6404 g, new design 1 produces 6924 g, and new design 2 achieves 7554 g. These figures clearly indicate a progressive increase in water production as the secondary heat source's input increases. In the base case, the system's performance was solely based on the solar chimney and solar still's inherent capabilities without any additional thermal energy input. The result is a baseline water production of 6404 g. With the introduction of a CSP system in new design 1, which heats the water stream by 20 °C at a flow rate of 30 kg/h, the water production rises to 6924 g. This increase can be attributed to the enhanced evaporation rate due to the higher water temperature in the basin, as observed in the previous temperature profile chart. The additional thermal energy from the CSP system boosted the overall efficiency of the desalination process. Further enhancement was observed in new design 2, where the water stream heated by 20 °C is increased to a flow rate of 60 kg/h. This design achieved the highest water production of 7554 g. The significant rise in water production compared to the base case and new design 1 underscored the positive impact of increased thermal energy input on the system's performance. By providing a larger quantity of preheated water, the new design 2 maximizes the evaporation rate, thereby producing more desalinated water.

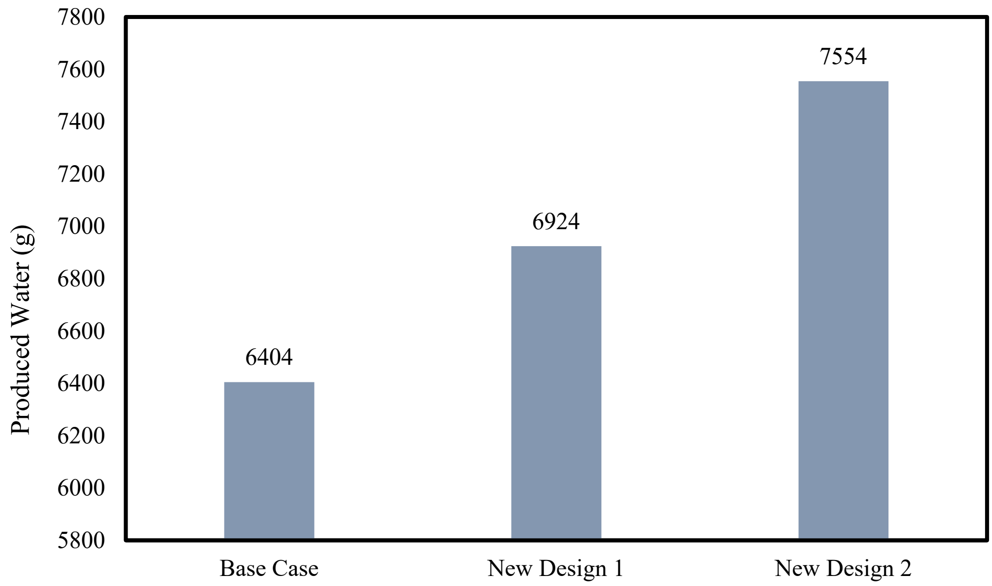

Figure 9. Water production achievement in 3 different cases.

On the other hand, the impact of additional heat from a CSP system on the inlet velocity of the chimney and the subsequent power generation in the hybrid solar chimney power plant (SCPP) and solar still system has been shown in Figure 10. In the base case, without additional heat input, the inlet velocity of the chimney is 1.85 m/s, resulting in a power output of 0.38 W. When additional heat is introduced in new design 1, which involves heating a water stream by 20 °C at a flow rate of 30 kg/h, the inlet velocity increases to 2 m/s, and the power output rises to 0.48 W. Further enhancement is observed in new design 2, where the heated water stream is increased to a flow rate of 60 kg/h, resulting in an inlet velocity of 2.2 m/s and a power output of 0.64 W.

The increase in chimney inlet velocity can be attributed to the added thermal energy from the CSP system. The rise in kinetic energy production is directly linked to the increased inlet velocity. As the velocity of the air entering the chimney increases, the kinetic energy available for driving the turbine also rises.

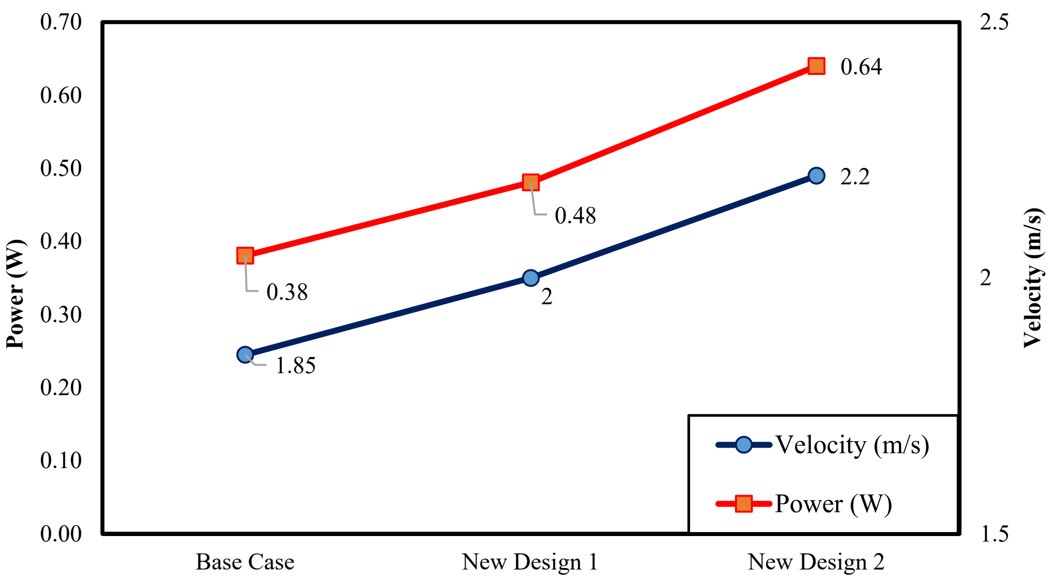

Figure 10. Effect of secondary heat source on velocity and kinetic power production.

Figure 11. shows the percentage change in power output and water production for the solar still system and hybrid Solar Chimney Power Plant (SCPP) when more heat from a concentrated solar power (CSP) system is added. The graph contrasts the new designs 1 and 2’s performance advantages with the base case. In new design

1, which involves heating a water stream by 20 °C at a flow rate of 30 kg/h, there is an 8.1% increase in water production and a 26.3% increase in power output. This indicated that even a modest addition of thermal energy from the CSP system can significantly enhance the system's performance. Even more notable gains may be seen in new design 2, which used a heated water stream with a higher flow rate of 60 kg/h. Power output soars by 68.2% while water production rises by 18%. This significant improvement demonstrates the favorable relationship between system performance and the amount of additional thermal energy. More warmed water is supplied to the system by the greater water flow rate, which greatly increases evaporation rates and desalination efficiency. The comparison between new design 1 and new design 2 clearly illustrates the benefits of integrating additional heat into the system.

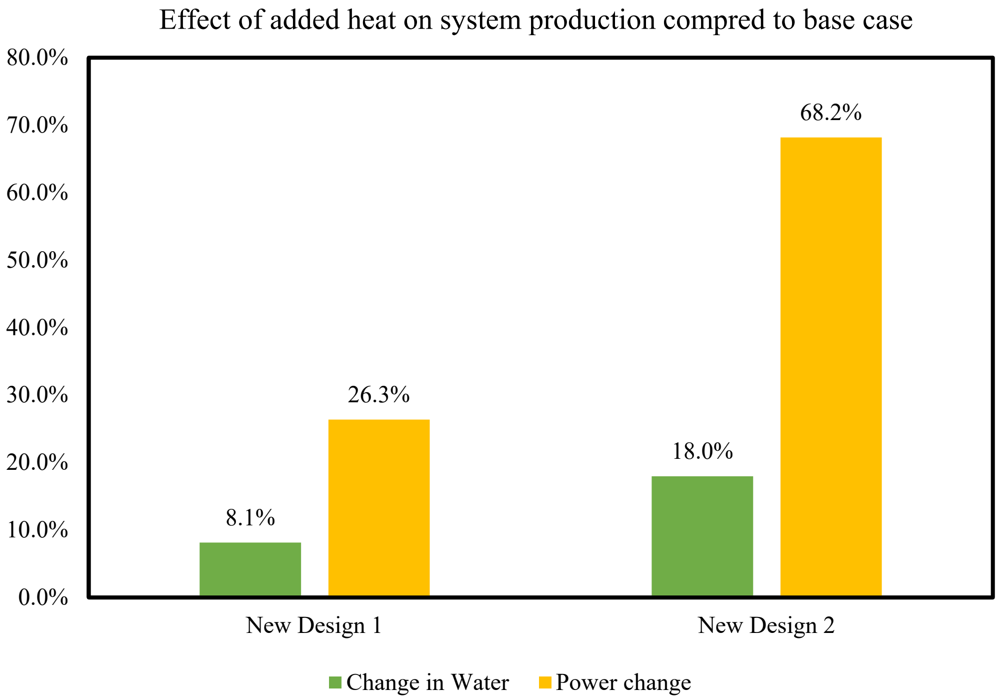

Figure 11. Effect of added heat on system production compared to base case.

4. Conclusions

Renewable energy sources, such as solar energy systems, are essential for mitigating the effects of global warming on water and electricity scarcity. The proposed triple integration of a solar chimney, a solar still, and a CSP system in the current work demonstrates a synergistic approach to achieving more sustainable water and electricity production. The CSP system's contribution of heat not only increases the temperature of the water in the solar still, thereby boosting desalinated water output, but also raises the air temperature entering the solar chimney, enhancing the updraft effect and resulting in higher turbine efficiency and electricity generation. This triple integration exemplifies a multifaceted solution that maximizes the use of solar energy, offering a promising pathway for sustainable and efficient use of resources. The key results of the study are summarized below:

- The basin water temperature reached approximately 78 °C, while the collector temperature in the basin reached to about 62 °C in the triple system, compared to the base case temperatures of around 73 °C and 58 °C, respectively.
- The amount of produced water increased from 6404 g in the base case to 7554 g in new design 2, showing 18% improvement in desalination efficiency.
- The inlet velocity of the chimney increased from 1.85 m/s in the base case to 2.2 m/s in new design 2, which corresponded to a rise in power output from 0.38 W to 0.64 W, corresponding to 68.2% increase in power production.
- The results proved that the effect of triple integration made a greater increase in power generation compared to water desalination

Finally, this paper demonstrated the triple hybrid system's performance and explained how it differs from a traditional solar chimney. Future research on the following topics appears to be required in the meantime to deepen our understanding of the system's actual performance:

(a) Conducting an experimental study for the intended triple integration system to provide a better understanding of various operating parameters
(b) Investigating scale-up aspects to evaluate the integrated design's viability and effectiveness in more extensive operational applications.
(c) Assessing the hybrid system's Levelized Cost of Energy (LCOE) to appropriately define its commercial features.

Author Contributions

M.S.: Project administration, Visualization, Formal analysis, Investigation, Writing—original draft; M.R.Y.: Project administration, Methodology, Conceptualization, Writing—review & editing; M.S.: Supervision, Methodology, Conceptualization; Y.B.: Writing—review & editing, Visualization. All authors have read and agreed to the published version of the manuscript.

Funding

This research received no external funding.

Institutional Review Board Statement

Not Applicable.

Informed Consent Statement

Not Applicable.

Data Availability Statement

The data supporting the findings of this study are available from the corresponding author upon reasonable request.

Acknowledgments

The authors would like to appreciate the Iran University of Science & Technology for its continual support during the research.

Conflicts of Interest

The authors declare no conflicts of interest.

Use of AI and AI-Assisted Technologies

During the preparation of this work, the authors used Grammarly and QuillBot solely for language editing, grammar correction, and paraphrasing. After using these tools, the authors reviewed and edited the content as needed and took full responsibility for the content of the published article.

Nomenclature

A	Area (m^2)	r	Radial coordinate (m)
C_P	Specific heat capacity of the air (J kg^{-1})	ΔT	The maximum change in temperature (K)
d	Distance (m)	T	Temperature (K)
g	Gravitational acceleration (m s^{-2})	u	Velocity in the radial direction (m s^{-1})
H	Chimney height (m)	V	Air velocity in the chimney (m s^{-1})
h	Coefficient of heat transfer (W/m2 ·K)	w	Velocity in the axial direction (m s^{-1})
k	Thermal conductivity (W/m.K)	z	Axial coordinate
L	Length (m)	β	Thermal expansion coefficient
$\dot{m}_h$	Fresh Water Production rate (kg/h)	α	Thermal diffusivity
Nu	Nusselt number	μ	Viscosity (Pa s^{-1})
P	Pressure (Pa)	ν	Kinematic Viscosity (m^2 s^{-1})

Pr	Prandtl number	ρ	The density of the air (Kg m^{-3})
P_e	Power (W)	ρ_0	Reference Density
Subscripts			
air	Air	ev	Evaporation
a	Ambient	h	Conduction Heat Transfer
c	Convective Heat Transfer	g	Glass Roof of Water Basin
ch	Chimney	w	Water
Acronym			
SCPP	Solar Chimney Power Plant	CSP	Concentrated Solar Power
CFD	Computational Fluid Dynamics	TES	Thermal Energy Storage

References

1. Mohammed, M.N.; Rashid, F.L.; Al-Obaidi, M.A.; et al. Recent advancement in hybrid solar chimney power plants: A comprehensive review of integration strategies and performance enhancements. *Int. Commun. Heat Mass Transf.* **2026**, *172*, 110492. https://doi.org/10.1016/j.icheatmasstransfer.2026.110492.
2. Hassan, Q.; Viktor, P.; J. Al-Musawi, T.; et al. The renewable energy role in the global energy Transformations. *Renew. Energy Focus* **2024**, *48*, 100545. https://doi.org/10.1016/j.ref.2024.100545.
3. Pontius, J.; McIntosh, A. Water Scarcity. In *Environmental Problem Solving in an Age of Climate Change: Volume One: Basic Tools and Techniques*; Pontius, J., McIntosh, A., Eds.; Springer International Publishing: Cham, Switzerland, 2024; pp. 87–103.
4. Alawad, S.M.; Mansour, R.B.; Al-Sulaiman, F.A.; et al. Renewable energy systems for water desalination applications: A comprehensive review. *Energy Convers. Manag.* **2023**, *286*, 117035. https://doi.org/10.1016/j.enconman.2023.117035.
5. McCulloch, M.T.; Winter, A.; Sherman, C.E.; et al. 300 years of sclerosponge thermometry shows global warming has exceeded 1.5 °C. *Nat. Clim. Chang.* **2024**, *14*, 171–177. https://doi.org/10.1038/s41558-023-01919-7.
6. Mehranfar, S., et al., Comparative assessment of innovative methods to improve solar chimney power plant efficiency. *Sustain. Energy Technol. Assess.* **2022**, *49*, 101807.
7. Kumar Mandal, D.; Biswas, N.; Manna, N.K.; et al. Impact of chimney divergence and sloped absorber on energy efficacy of a solar chimney power plant (SCPP). *Ain Shams Eng. J.* **2024**, *15*, 102390. https://doi.org/10.1016/j.asej.2023.102390.
8. Mandal, D.K.; Gupta, K.K.; Biswas, N.; et al. Sustainable design of solar chimney power plants: A hybrid neural network approach for thermo-economic optimization. *Renew. Energy* **2026**, *256*, 124154. https://doi.org/10.1016/j.renene.2025.124154.
9. Haaf, W.; FRIEDRICH, K.; MAYR, G.; et al. Solar chimneys part I: Principle and construction of the pilot plant in Manzanares. *Int. J. Sol. Energy* **1983**, *2*, 3–20. https://doi.org/10.1080/01425918308909911.
10. Saleh, M.J.; Atallah, F.S.; Algburi, S.; et al. Enhancement methods of the performance of a solar chimney power plant: Review. *Results Eng.* **2023**, *19*, 101375. https://doi.org/10.1016/j.rineng.2023.101375.
11. Ghalamchi, M.; Kasaeian, A.; Ghalamchi, M.; et al. An experimental study on the thermal performance of a solar chimney with different dimensional parameters. *Renew. Energy* **2016**, *91*, 477–483. https://doi.org/10.1016/j.renene.2016.01.091.
12. Gholamalizadeh, E.; Kim, M.H. CFD (computational fluid dynamics) analysis of a solar-chimney power plant with inclined collector roof. *Energy* **2016**, *107*, 661–667. https://doi.org/10.1016/j.energy.2016.04.077.
13. Nasraoui, H.; Driss, Z.; Kchaou, H. Novel collector design for enhancing the performance of solar chimney power plant. *Renew. Energy* **2020**, *145*, 1658–1671. https://doi.org/10.1016/j.renene.2019.07.062.
14. Al-Abadi, A.K.; Kridi, A.F.; Hussain, G.F.M. Comparison between simulated and calculated power of the solar chimney with black concrete base using ANSYS program. *Al-Qadisiya J. Eng. Sci.* **2010**, *3*, 347–364.
15. Afsari, H. Experimental and numerical study on effects of additional air height and existing soil layer under the collector of solar chimney. *Energy Syst.* **2024,** 1–7.
16. Li, Y.; Liu, S.; Lu, J. Effects of various parameters of a PCM on thermal performance of a solar chimney. *Appl. Therm. Eng.* **2017**, *127*, 1119–1131. https://doi.org/10.1016/j.applthermaleng.2017.08.087.
17. Ahmed, O.K.; Algburi, S.; Ali, Z.H.; et al. Hybrid solar chimneys: A comprehensive review. *Energy Rep.* **2022**, *8*, 438–460. https://doi.org/10.1016/j.egyr.2021.12.007.
18. Mokrani, O.B.E.K.; Ouahrani, M.R.; Sellami, M.H.; et al. Experimental investigations of hybrid: Geothermal water/solar chimney power plant. *Energy Sources Part A Recovery Util. Environ. Eff.* **2024**, *46*, 15474–15491.
19. Pratap Singh, A.; Kumar, A.; Akshayveer; et al. Performance enhancement strategies of a hybrid solar chimney power plant integrated with photovoltaic panel. *Energy Convers. Manag.* **2020**, *218*, 113020. https://doi.org/10.1016/j.enconman.2020.113020.
20. Abdelsalam, E.; Almomani, F.; Kafiah, F. Integrating solar chimney power plant with electrolysis station for green hydrogen production: A promising technique. *Int. J. Hydrogen Energy* **2024**, *52*, 1550–1563.

21. Sajjadi, M.; Shirvani, M.; Yousefi, M.R.; et al. Day and Night Times Performance Improvement of the Solar Chimney by Combining with the CSP System. *Appl. Sol. Energy* **2021**, *57*, 310–322. https://doi.org/10.3103/s0003701x21040095.
22. Abdelsalam, E.; Almomani, F.; Kafiah, F.; et al. A case study of an integrated solar chimney power plant and water desalination plant in Qatar. *Desalination* **2024**, *575*, 117283. https://doi.org/10.1016/j.desal.2023.117283.
23. Cooper, P.I. Digital simulation of transient solar still processes. *Sol. Energy* **1969**, *12*, 313–331. https://doi.org/10.1016/0038-092x(69)90046-2.
24. Zuo, L.; Yuan, Y.; Li, Z.; et al. Experimental research on solar chimneys integrated with seawater desalination under practical weather condition. *Desalination* **2012**, *298*, 22–33. https://doi.org/10.1016/j.desal.2012.05.001.
25. Mostafa, M.; Abdullah, H.M.; Mohamed, M.A. Modeling and experimental investigation of solar stills for enhancing water desalination process. *IEEE Access* **2020**, *8*, 219457–219472. https://doi.org/10.1109/access.2020.3038934.
26. Long, T.; Zheng, D.; Li, Y.; et al. Experimental study on liquid desiccant regeneration performance of solar still and natural convective regenerators with/without mixed convection effect generated by solar chimney. *Energy* **2022**, *239*, 121919. https://doi.org/10.1016/j.energy.2021.121919.
27. Kabeel, A.E.; Omara, Z.M.; Essa, F.A. Enhancement of modified solar still integrated with external condenser using nanofluids: An experimental approach. *Energy Convers. Manag.* **2014**, *78*, 493–498. https://doi.org/10.1016/j.enconman.2013.11.013.
28. Huang, W.; Gao, X.; Sun, L.; et al. Black g-C3N4-based hydrogel for water evaporation and photothermal persulfate activation. *J. Mater. Sci. Technol.* **2026**, *249*, 153–163. https://doi.org/10.1016/j.jmst.2025.06.014.
29. Afsari, H.; Yousefi, M.R.; Sajjadi, M.; et al. Experimental and Numerical Study on the Integrated Solar Chimney System with Solar Still for Water Desalination. *Energy Technol.* **2023**, *11*, 2300462. https://doi.org/10.1002/ente.202300462.
30. Gevorkov, L.; Domínguez-García, J.L.; Rassõlkin, A.; et al. Comparative Simulation Study of Pump System Efficiency Driven by Induction and Synchronous Reluctance Motors. *Energies* **2022**, *15*, 4068. https://doi.org/10.3390/en15114068.
31. Ayadi, A.; Driss, Z.; Bouabidi, A.; et al. Experimental and numerical study of the impact of the collector roof inclination on the performance of a solar chimney power plant. *Energy Build.* **2017**, *139*, 263–276. https://doi.org/10.1016/j.enbuild.2017.01.047.
32. Kasaeian, A.; Ghalamchi, M.; Ghalamchi, M. Simulation and optimization of geometric parameters of a solar chimney in Tehran. *Energy Convers. Manag.* **2014**, *83*, 28–34. https://doi.org/10.1016/j.enconman.2014.03.042.
33. Dunkle, R. Solar water distillation: The roof type still and a multiple effect diffusion still. in Proc. International Heat Transfer Conference, University of Colorado, USA. 1961.
34. Agrawal, A.; Rana, R.; Srivastava, P.K. Heat transfer coefficients and productivity of a single slope single basin solar still in Indian climatic condition: Experimental and theoretical comparison. *Resour. Effic. Technol.* **2017**, *3*, 466–482. https://doi.org/10.1016/j.reffit.2017.05.003.
35. Sakonidou, E.; Karapantsios, T.D.; Balouktsis, A.I.; et al. Modeling of the optimum tilt of a solar chimney for maximum air flow. *Sol. Energy* **2008**, *82*, 80–94. https://doi.org/10.1016/j.solener.2007.03.001.